AD-A139 253 A REASSESSMENT OF THE MEASUREMENT UNCERTAINTY OF THE XT-90 TWIN T DUAL AD..(U) ROYAL SIGNALS AND RADAR ESTABLISHMENT MALVERN (ENGLAND) G J SLACK ET AL. 1983 1/1

UNCLASSIFIED RSRE-MEMO-3832 DRIC-BR-90881 F/G 9/5 NL

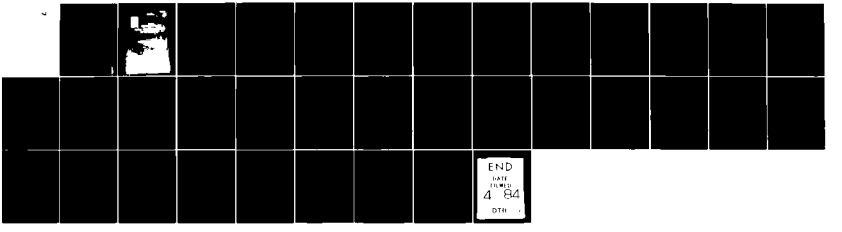

END
DATE FILMED
4 84
DTIC

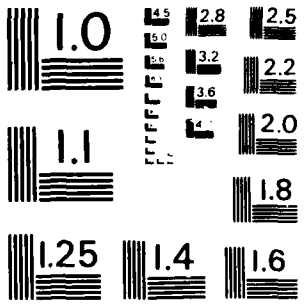

MICROCOPY RESOLUTION TEST CHART
NATIONAL BUREAU OF STANDARDS - 1963 - A

ROYAL SIGNALS AND RADAR ESTABLISHMENT

Memorandum 3632

TITLE: A REASSESSMENT OF THE MEASUREMENT UNCERTAINTY OF THE XT-90 TWIN T DUAL ADMITTANCE BRIDGE

AUTHORS: G J Slack and T N W Graham

DATE:

SUMMARY

This memorandum supplements and updates the original report on the Twin T Bridge which was written over thirty years ago.

An explanation of both the practical and theoretical circuit development is given leading up to an equivalent circuit and the bridge balance difference equations. A brief description of the calibration procedures used is given, together with details of the method used to measure standards at RSRE. Finally a new assessment of overall bridge measurement uncertainty has been made, and a single equation for this produced for each of the three frequencies at which standards are currently calibrated.

RSRE MEMORANDUM No 3632

A REASSESSMENT OF THE MEASUREMENT UNCERTAINTY OF THE XT-90 TWIN T DUAL ADMITTANCE BRIDGE

G J Slack and T N W Graham

LIST OF CONTENTS

1. Introduction
2. Basic Bridge Circuit
3. Practical Bridge Circuit
4. Final Balance Difference Equations as defined by Woods
5. Capacitance Standards
6. Equipment and Measurement Procedure used with the Bridge at RSRE
7. Calibration Procedure for the *Shunt Elements*
8. Calibration Procedure for the Series Elements
9. Final Balance Difference Equations used with the Bridge at RSRE
10. Assessment of the Bridge Measurement Uncertainty
11. Conclusions

LIST OF TABLES

1. Calculated and Measured Values of the Standard Capacitors.
2. Uncertainty of Measuring Capacitors C_a and C_b.
3. List of Components of Uncertainty contributing towards the Bridge Overall Measurement Uncertainty.
4. Single Equations of Bridge Overall Measurement Uncertainty.
5. Measured Uncertainty Figures for all standards having a Minimum Conductance and Capacitance of 1 mS and 0.15 pF respectively.
6. Measured Uncertainty Figures for Standard Capacitors.

LIST OF FIGURES

Fig. 1 Basic Bridge Circuit Configuration.
Fig. 2 Basic Circuit as Connection of Two T-Networks
Fig. 3 Basic Circuit Components
Fig. 4 Transfer Impedance "A" Arm
Fig. 5 First Stage towards Practical Circuit
Fig. 6 Complete Woods Equivalent Circuit
Fig. 7 Effect of Common and Mutual Earth Impedances
Fig. 8 Revised Configuration of Standard Capacitors
Fig. 9 Bridge Adapter to GR900 Connector
Fig. 10 Circuit Arrangement for Measuring Shunt Residuals g_a and g_b

1. INTRODUCTION

The RSRE XT-90 Twin T Dual Admittance Bridge, commonly called the Woods bridge after its designer, operates over the frequency range from 5 MHz to 200 MHz and is capable of measuring each component of an unknown admittance, within the range zero to 50 pF and/or zero to 50 mS. The main purpose of this memorandum is to describe both the developments carried out and measurement methods used on the bridge at RSRE in order to update the original report [1] and produce a reassessment of the bridge measurement uncertainty. A simpler explanation of the bridge circuit design has also been included (Sections 2, 3 and 4) since the quantity and intensity of information in [1] is usually found to be rather overwhelming; it should be stressed however that this explanation only supplements and does not replace the full report.

The bridge was designed over 30 years ago, at the then Aeronautical Inspection Directorate (A.I.D.) Harefield, Middlesex and was built by KGM Electronics Ltd. Since then the bridge has been used to provide top echelon standard measurements of admittance in coaxial line and is at present located in L4 Division (r.f. and microwave standards) at RSRE. Work on two other similar bridges is also continuing at the National Physical Laboratory, Teddington [2] and the Electrical Quality-Assurance Directorate.

Since frequent reference will be made to [1] in this memorandum the designation (A.I.D.) will be used for convenience.

2. BASIC BRIDGE CIRCUIT

The basic circuit configuration of the VHF Twin T Admittance Bridge is shown in fig. 1 and can be seen to consist of two separately identifiable T-networks (hence the name Twin-T) connected in parallel between an R.F. source and detector (see also fig. 2). The two T-networks will be referred to as the A arm and B arm networks for convenience. Each of the bridge shunt elements (impedances Z_3 and Z_6) includes a precision standard variable capacitor but the remaining four impedances (series elements) are of fixed value. Before a device under test (DUT) is connected for measurement, these standard capacitors are adjusted to obtain a null at the detector output, so ensuring zero-transmission between the source and detector and leaving the bridge in an initial referenced state. After a DUT has been connected in parallel with Z_6, the bridge is rebalanced by adjusting the standard capacitors to re-establish this zero transmission condition, so that the measured value for the DUT is calculated from the observed change in each capacitor.

The components chosen for the basic circuit are shown in fig. 3, where C_1 corresponds to Z_1 in fig. 1, L_a, $g_a$and C_a (precision variable) to Z_3, C_2 to Z_2, C_3 to Z_4, L_b, g_b and C_b (precision variable) to Z_6 and finally G_s to Z_5. The The elements g_a and g_b represent shunt losses associated mainly with the inductors L_a and L_b respectively. It should be noted that although the principal measurement terminals are on the B arm, a similar set exists on the A arm mainly for the purpose of measuring unwanted circuit residuals to be discussed later.

In order to determine the admittance of the DUT from the changes in C_a and C_b, and analysis of the bridge zero transmission balance conditions is required. From fig. 4 the transfer impedance Z_{ta} of the A arm, defined as the input voltage V_{in} divided by the output current with the output terminals short circuited, is given by

$$Z_{ta} = Z_1 + Z_2 + Z_1 Z_2/Z_3 \qquad (1)$$

Similarly for the B arm

$$Z_{tb} = Z_4 + Z_5 + Z_4Z_5/Z_6 \tag{2}$$

The condition for zero transmission through the bridge circuit is then given by

$$Z_{ta} + Z_{tb} = 0 \tag{3}$$

Applying (1), (2) and (3) to the circuit of fig. 3 gives the following balance equations

$$\frac{1}{w^2L_a} = C_a + C_1 + C_2 + \frac{C_1C_2}{C_3}\left(1 + \frac{g_b}{G_s}\right) \tag{4}$$

$$\frac{1}{w^2L_b} = C_b + C_3\left(1 - \frac{g_aG_s}{w^2C_1C_2}\right) \tag{5}$$

where $g_a \approx g_b \ll G_s$

Using both (4) and (5) for the cases of initial bridge balance (ie. measurement terminals open circuited) and then final balance (with DUT connected) gives the following expressions (the balance difference equations) for the unknown DUT admittance ($Y_x = G_x + jwC_x$) in terms of C_a and C_b.

DUT connected to B arm measurement terminals

$$G_{xb} = \frac{C_3G_s}{C_1C_2}(C_{a1} - C_{a2}) \tag{6}$$

$$C_{xb} = (C_{b1} - C_{b2}) \tag{7}$$

where C_{a1} and C_{b1} are the initial values, and C_{a2} and C_{b2} are the final values of C_a and C_b, and subscript b on both G_x and C_x relates to measurements made on the B arm.

DUT connected to A arm measurement terminals

$$G_{xa} = -w^2\frac{R_sC_1C_2}{C_3}(C_{b1} - C_{b2}) \tag{8}$$

$$C_{xa} = (C_{a1} - C_{a2}) \tag{9}$$

where subscript a on both G_x and C_x relates to measurements made on the A arm, and $R_s = 1/G_s$.

Both the derivation of these equations and an explanation for the particular choice of components shown in fig. 3 are given in [A.I.D.] sections 2.6 - 5.1, pages 3-9.

In order to gain a better understanding of how the bridge circuit operates it is worth considering equations (4) to (9) further. An examination of equations (6) and (7) shows that for an unknown admittance Y_{xb} connected to the B arm measurement terminals, the capacitive element of that admittance, C_{xb}, causes a change only in the B arm capacitor C_b (ie. the same arm) whereas the conductive element, G_{xb}, changes only the A arm capacitor C_a (ie. the opposite arm). A similar situation exists for measurements made on the A arm terminals. This lack of interaction between the two precision variable capacitors is an important feature of the bridge circuit and enables rapid balancing to be achieved during measurement. The simple forms of both (7) and (9) are logical since any susceptance (ie. positive or negative capacitance) connected across the A or B arm terminals can be directly compensated for by altering C_a or C_b respectively. The situation for conductance is not easily seen, but notice that equations (6) and (8) can be derived simply from (4) and (5) in that placing a conductance across either terminal will increase g_a or g_b accordingly. Because the measured admittance of the DUT is expressed in terms of C_1, C_2, C_3, G_s and changes in C_a and C_b, these are referred to as the dependent circuit elements and are required to have long term stability in order to maintain calibration. L_a and L_b, which do not appear in equations (6) to (9), are called the independent elements and need only have short term stability between initial and final bridge balance. In practice, L_a and L_b take the form of a set of plug-in inductors, an appropriate pair being chosen and connected to the bridge for the particular frequency of measurement.

The balance equations (4) and (5) both have the form:

$$\frac{1}{w^2 L} = C \qquad (10)$$

which suggests a resonant type behaviour. It can be shown ([A.I.D.] section 9.2, pages 27-29) that for bridge balance at frequencies greater than approximately 50 MHz, transmission through both A and B arms is near resonant maximum even though the detector output is nulled. This explains the very high level of discrimination ie. 2 parts in 10^5 obtained from this circuit. However for lower frequencies the term $g_a G_s / w^2 C_1 C_2$ in (5) becomes greater than unity requiring larger values of C_b to maintain balance. This causes the B arm network to depart from near resonant transmission at bridge balance and is accompanied by a significant deterioration in its discrimination. At frequencies below 5 MHz L_b is no longer required (making $L_b = \infty$), C_b is made very large ($\approx$ 400 pF) with the use of external capacitors and the B arm discrimination drops to 0.05 pF or 1 part in 10^3. The A arm meanwhile is unaffected in this way and maintains its full discrimination (2 parts in 10^5) over the whole frequency range.

The measurement range of the bridge can be calculated from the component values given in fig. 3. For the B arm terminals the capacitance range is 50 pF (equation (7)) and the conductance range is zero to 50 mS from equation (6). For the A arm terminals the capacitance range is 25 pF (equation (9)) whereas the conductance range is frequency dependent, covering zero to 40 mS at 200 MHz and yet only zero to 0.1 mS at 10 MHz (equation (8)). The B arm terminals are therefore more commonly used because of their greater measurement range although the A arm does offer significantly greater discrimination when measuring low loss devices at low frequencies (eg. dielectric loss measurements).

3. PRACTICAL BRIDGE CIRCUIT

The practical circuit is more complex than as shown in fig. 3, firstly because of certain bridge operational requirements and secondly in order to allow for the effects of component residuals. A first stage towards describing the full circuit is shown in fig. 5 which has been drawn in keeping with [A.I.D.] but still has the same form as fig. 3. The bridge shunt elements now include inductors ℓ_{a1}, ℓ_{a2}, ℓ_{b1}, ℓ_{b2} and capacitors C_{at}, C_{at1}, C_{bt} and C_{bt1}; the series capacitors C_1, C_2 and C_3 each have associated residual inductance and G_s is shunted by residual capacitance C_s.

When performing a measurement using the B arm terminals the auxiliary variable capacitors C_{bt} (coarse adjustment) and C_{bt1} (fine adjustment) are used to obtain initial bridge balance instead of the precision capacitor C_b. This enables C_b to be set to a convenient initial reference position and allows its full capacitance change, in either a positive or negative direction to be used if required during measurement. Variable capacitors C_{bt} and C_{bt1} are in fact used in two different circuit configurations; below 180 MHz the inductors ℓ_{b1} and ℓ_{b2} have negligible effect therefore placing these capacitors directly in parallel with L_b and C_b. Above 180 MHz however it is difficult to make L_b small enough to suit the balance requirement of equation (5) and so the circuit comprising C_{bt}, C_{bt1}, ℓ_{b1} and ℓ_{b2} is used with L_b removed altogether. This circuit is operated above series resonance in order to offer a small positive (inductive) reactance, although care must be taken to avoid actual series resonance and the resulting false balance condition. Operation of the A arm is similar to that explained in this paragraph for the B arm.

It can be seen from equations (6) and (8) that the series capacitors C_1, C_2 and C_3 appear only in the form C_3/C_1C_2. If the value of this term can be maintained relatively constant then errors in the individual capacitance values, which result from residual series inductance and can be several per cent at 200 MHz, are of no concern. By choosing $C_1 = C_2 = \frac{1}{2} C_3$ and arranging for the residual inductance of C_1 and C_2 ($L_h + \ell$ in fig. 5) to be slightly greater than that of C_3 (ie. L_h) then it can be shown ([A.I.D.] section 12.2 pages 33-34) that a compensation effect occurs and the resulting variation of C_3/C_1C_2 from its zero frequency value is less than 3 parts in 10^4 at 200 MHz.

In order to correct the errors introduced by the residual shunt capacitance C_s, the bridge circuit has to be reanalysed treating the resistor G_s now as an admittance $G_s + jwC_s$. The resulting new balance difference equations are given below.

DUT connected to B arm measurement terminals

$$G_{xb} = \frac{C_3 G_s}{C_1 C_2} \Delta C_a \qquad (11)$$

$$C_{xb} = \Delta C_b + \frac{G_{xb}}{G_s} C_s \qquad (12)$$

where $\Delta C_a = (C_{a1} - C_{a2})$ and $\Delta C_b = (C_{b1} - C_{b2})$

DUT connected to A arm measurement terminals

$$G_{xa} = \frac{-w^2 C_1 C_2}{C_3 G_s \left(1 + \frac{w^2 C_s^2}{G_s^2}\right)} \Delta C_b \qquad (13)$$

$$C_{xa} = \Delta C_a - \frac{G_{xa}}{G_s} C_s \qquad (14)$$

Equation (11) shows that G_{xb} is unaffected by introducing C_s (ie. equations (6) and (11) are identical) whereas for conductance measurements across the A arm (equation (13)), R_s in equation (8) has been replaced by the term $1/G_s\ (1 + w^2C_s^2/G_s2)$ namely the equivalent series resistance of the admittance $G_s + jwC_s$. Equations (12) and (14) show that C_{xb} and C_{xa} both now include a term in C_s similar in magnitude but of opposite sign. This feature enables C_s to be determined as part of the calibration procedure to be discussed later. More information on this practical circuit as well as a detailed description of the mechanical design of the Twin T bridge are given in [A.I.D.] sections 5.2 - 6.5 pages 9-17. It should be noted that each bridge terminal has a coaxial form for reasons explained in [A.I.D.] section 2.5 pages 2-3 and that on the RSRE bridge a terminal adaptor has been added (to be described later) in order to create a measurement plane in terms of the now common GR900 precision coaxial connector.

The full equivalent circuit as originally derived by Woods is shown in fig. 6 where the residual inductances associated with the series capacitors C_1, C_2 and C_3 have not been included since they do not appear in the final circuit balance difference equations; their intended effect being to maintain the term C_3/C_1C_2 virtually frequency independent as explained earlier. The circuit contains a further number of residual terms as listed below.

(i) The common junction equivalent inductances L_j and L_k (both arms)

If the junction between three or more elements has finite area then a common junction impedance exists and the elements cannot be modelled as being connected together at one single point. To allow for this effect at junctions 1 and 2 in fig. 5 the inductances L_j and L_k have been added, their corresponding values being the same for each arm as a result of bridge symmetry. As shown in fig. 6, the B arm nodes adjacent to L_j and L_k have been termed $\overline{B}$, $\overline{\overline{B}}$ and $\overline{\overline{\overline{B}}}$ (expressed as 1-bar, 2-bar and 3-bar points respectively) both for future reference and to remain in keeping with [A.I.D.]. A similar form of notation is also used on the A arm.

Further information on the equivalent circuit of these junctions, leading to the choice of L_j and L_k, is given in [A.I.D.] section 15.6.1 - 15.6.3 pages 59-60.

(ii) The common and mutual earth junction impedances

The principle of common junction impedance referred to in (i) above will also apply to the earth junction E. In fact the full equivalent circuit of the bridge is more complex than as shown in fig. 6, taking the form of fig. 7 (where the shunt elements have been diagrammatically

simplified for convenience and the bridge resistor has been redrawn to expose its residual inductance L_s). The bridge has been designed such that a mutual impedance Z_m exists between each common earth junction inductance L_g and one of the residual inductances associated with the bridge series elements C_1, C_2, C_3 and G_s. By choosing the magnitude of Z_m to cancel out each L_g element, an effective earth junction is created at a single point thus making the circuit of fig. 6 valid. The residual inductance of each series element will also be reduced by an amount L_g although this does not affect the frequency compensation of C_3/C_1C_2 because each inductance is reduced by the same amount. The equivalent shunt capacitance C_s associated with G_s in fig. 5 has however been renamed C_{sg} in fig. 6 in order to emphasise the influence of Z_m on L_s. More information on this general topic can be found in [A.I.D.] section 12.4.1 page 36.

(iii) Residuals associated with the standard capacitors C_a and C_b

Each bridge standard capacitor has associated residuals in the form of one fixed and one variable inductance and one loss resistor ie. L_{ob}, L_{cb} and R_{ob} respectively for the B arm capacitor.

(iv) Bridge coaxial terminals

Each bridge coaxial terminal section is modelled in terms of the equivalent lumped circuit components L_t and C_t. Note that on the RSRE bridge these have to be augmented to allow for the adaptor to GR900 coaxial connector (to be described later).

(v) Terminal fringe capacitance C_f (both arms)

At initial balance each terminal is left open circuited in order to reference the bridge to a nominally zero admittance. The resulting distortion of the electric field at this open ended coaxial measurement plane can be represented by the equivalent lumped capacitance C_f.

4. FINAL BALANCE DIFFERENCE EQUATIONS AS DERIVED BY WOODS

A general analysis of the circuit in fig. 6 is required in order to derive a relationship between the unknown admittance of a DUT connected at the measurement terminals and the observed changes in C_a and C_b. This full analysis commences in [A.I.D.] sections 12.4.2 to 14.3 pages 37-49, where the balance difference conditions at the bridge 3-bar points are established, followed by [A.I.D.] sections 15.6.4 to 16.4 pages 60-64, where the necessary conditions are referred to the 1-bar points producing the 1-bar balance difference equations given below.

DUT connected to the B arm measurement terminals

$$G_{xb} = \frac{G_s C_3}{C_1 C_2}\,\Delta\bar{C}_a \left| 1 + w^2 L_j(2\bar{C}_{b2} - \bar{C}_{a1} - \bar{C}_{a2} - C_5) - w^2 L_k(\Delta\bar{C}_a + C_5) \right.$$
$$\left. -2(L_j + L_k)\left(\frac{C_3 g_a G_s}{C_1 C_2} + \frac{w^2 C_1 C_2 g_b}{C_3 G_s}\right)\right| + w^2 R_{ob}(\bar{C}_{b1}^2 - \bar{C}_{b2}^2) \qquad (15)$$

$$\bar{C}_{xb} = \Delta\bar{C}_b + \frac{\bar{G}_{xb}\,C_{sg}}{G_s} + (L_j + L_k)\bar{G}_{xb}^2 + 2(L_j + L_k)g_b\bar{G}_{xb} - 2L_k g_a \bar{G}_{xb} - \frac{R_{oa}C_3}{R_s C_1 C_2}\,(\bar{C}_{a1}^2 - \bar{C}_{a2}^2) + C_f \qquad (16)$$

where $C_5 = 2(C_1 + C_2 + \frac{C_1C_2}{C_3} - C_3)$

$= 5$ pF

DUT connected to the A arm measurement terminals

$$\bar{G}_{xa} = -w^2R_s\,\frac{C_1C_2}{C_3}\,\Delta\bar{C}_b\Big\{1 + w^2L_j\,(2\bar{C}_{a2} - \bar{C}_{b1} - \bar{C}_{b2} + C_5) + w^2L_k(C_s - \Delta\bar{C}_b) + 2(L_j + L_k)\Big(\frac{C_3g_aG_s}{C_1C_2} + \frac{w^2C_1C_2g_b}{C_3G_s}\Big)\Big\} + w^2R_{oa}(\bar{C}_{a1}^2 - \bar{C}_{a2}^2) \qquad (17)$$

$$\bar{C}_{xa} = \Delta\bar{C}_a - \frac{\bar{G}_{xa}}{G_s}\,C_{sg} + (L_j + L_k)\bar{G}_{xa}^2 + 2(L_j + L_k)g_a\,\bar{G}_{xa} - 2L_k g_b\,\bar{G}_{xa} - w^2\,\frac{R_{ob}C_1C_2}{G_sC_3}\,(\bar{C}_{b2}^2 - \bar{C}_{b1}^2) + C_f \qquad (18)$$

These four equations, repeated here for convenience, correspond to [A.I.D.] equations (128), (129), (132) and (133) respectively. Note that the R.H.S. of equation (17), unlike its [A.I.D.] counterpart, has a negative sign associated with both its $\Delta\bar{C}_b$ terms; this maintains the definition $\Delta\bar{C}_b = (\bar{C}_{b1} - \bar{C}_{b2})$ for measurements made on either terminal and avoids the confusion of having $\Delta C_b = (\bar{C}_{b1} - \bar{C}_{b2})$ for B arm terminal measurements, but $\underline{\Delta\bar{C}_b} = (\bar{C}_{b2} - \bar{C}_{b1})$ for those on the A arm, as is used in [A.I.D.]. The terms $\bar{G}_{xb}$ and $\bar{C}_{xb}$ above (or equally $\bar{G}_{xa}$ and $\bar{C}_{xa}$ for the A arm) represent changes in conductance and capacitance occurring at the 1-bar points between initial and final bridge balance. These changes then have to be transferred through the corresponding terminal section to give the final required G_x and C_x values of the unknown admittance Y_x. The circuit elements C_{bt}, C_{bt1}, ℓ_{b1}, ℓ_{b2} and L_b (taking the B arm as an example), which are physically contained within the secondary block of the bridge, do not appear in equations (15) to (18) and are therefore independent elements. This does not apply to L_{cb} and L_{ob} because they are considered effectively part of C_b.

In order for the bridge to make precision admittance measurements, values for the relevant components and residuals in fig. 6 need to be accurately determined. This forms the bridge calibration procedure which will be described in sections 7 and 8 of this report. It should be noted that for the RSRE bridge some of these procedures differ from those originally developed by Woods and have resulted in changes to the balance difference equations (15) to (18).

5. CAPACITANCE STANDARDS

Most of the Twin T bridge calibration procedures require the use of coaxial capacitance standards of the type described in [A.I.D.] section 8.1 pages 21-24. Further work at RSRE has resulted however in the following changes being made to the fundamental assessment and practical use of these standards.

(a) The zero frequency capacitance is calculated using the formula given below.

$$C = \frac{0.24176}{\log_{10}\left(\frac{R_o}{R_i}\right)} \text{ pF/cm at } 20^{\circ}C, \text{ 760 mmHg } (0^{\circ}C) \text{ and 50\% R.H.} \qquad (19)$$

where an allowance has been made for an air dielectric relative h ..ity of 50% [3] which results in a capacitance value approximately 1 part in 10^4 higher than for the corresponding [A.I.D.] equation (9). Note that in this [A.I.D.] equation, the length L is expressed in centimetres not inches.

(b) The standard capacitors are measured at a frequency of 1 kHz using and A.F. inductive ratio capacitance bridge. This seems a more direct method than that in [A.I.D.] where the 4.5 MHz measurement is based on an A.F. calibration of C_a and C_b and assumes that at 4.5 MHz the effects of residuals in the latter will be negligible.

The capacitance of each standard has been calculated from equation (19), using mean physical dimensions each with an associated uncertainty of $\pm$ 0.002 μm, and is compared with the measured A.F. values in Table 1.

TABLE 1

CALCULATED AND MEASURED VALUES OF THE STANDARD CAPACITORS

Capacitor	Calculated Capacitance (pF)		Measured Capacitance at 1 kHz (pF)		Difference (pF)
	Mean	Uncertainty	Mean	Uncertainty	
C_{s10}	2.6211	$\pm$ 0.0020	2.6230	$\pm$ 0.0003	-0.0019
C_{s11}	5.2088	$\pm$ 0.0037	5.2108	$\pm$ 0.0005	-0.0020
C_{s12}	10.4521	$\pm$ 0.0071	10.4602	$\pm$ 0.0010	-0.0081
C_s13	20.9072	$\pm$ 0.0140	20.9238	$\pm$ 0.0021	-0.0166

Table 1 shows that the measured values have significantly smaller associated uncertainty limits and the R.F. capacitance calculations for each standard have therefore been based on these measured values. The slight discrepancy between the measured and calculated values, particularly for C_{s12} and C_{s13}, suggests that further examination of the metrology procedure used with these capacitors is required.

(c) The capacitors are used with their outer conductors extended by at least twice their bore diameter as shown in fig. 8. This firstly prevents significant radiation of energy, which could interact with local objects such as the operator's hands and disturb the measurement, and secondly defines more precisely the fringe capacitance C_f, resulting in a calculated value [4] of 0.398 pF.

For the sake of completeness it is worth mentioning here that [A.I.D.] equations (10) and (12) are used to calculate the change in R.F. capacitance produced at the bridge terminals on connecting a capacitance standard, and the equation at the top of [A.I.D.] page 75 is used to transform this change to the bridge 1 bar points to which the calibrations of the precision variable capacitors C_a and C_b are referred.

6. EQUIPMENT AND MEASUREMENT PROCEDURE USED WITH THE RSRE BRIDGE

The RSRE bridge is driven from a crystal controlled synthesised R.F. signal generator, used normally with an output power of approximately 8 mW, having a long term drift rate of $\pm$ 3 parts in 10^9 per day and an absolute accuracy, assessed with a frequency counter referenced to an RSRE frequency standard, of better then $\pm$ 3 parts in 10^6. Bridge balance is detected using a spectrum analyser which has a maximum sensitivity of -117 dBm ($\approx$ 300 nV) and whose frequency range enables it to replace the three separate and somewhat cumbersome communications receivers used previously. Both the R.F. source and detector are connected to the bridge via semi-rigid cable and N type or TNC connectors in order to minimise R.F. leakage. To maintain system accuracy and stability the bridge is situated in a laboratory which is temperature controlled at $20^oC \pm 1^oC$ and humidity controlled to 50% $\pm$ 15% R.H., the exact values being regularly checked by a calibrated thermometer and hygrometer respectively.

7. CALIBRATION PROCEDURES FOR THE SHUNT ELEMENTS

(i) Precision Variable Capacitors C_a and C_b (including L_{oa}, L_{ca}, L_{ob}, L_{cb})

It can be seen from [A.I.D.] Table 6 page 74 that the measured values for standard capacitor C_{s10} vary with initial micrometer setting, deviations from the mean value being more than 1% for C_b and 0.5% for C_a. In an attempt to smooth out these large variations a new calibration procedure was developed. This is very comprehensive, the final calibration for each frequency being produced from parts of several separate calibration runs. A large computer program has been developed to achieve this and a laboratory report on how to form a calibration using this program is being produced for future use.

In order to give some idea of the steps involved, the main stages in calibrating one capacitor at one frequency are described below taking C_b as the example.

(a) The bridge is balanced with C_b set to one extreme end of its micrometer operating range.

(b) Capacitor C_{s10} is connected to the bridge terminals producing a known change of capacitance at the 1 bar points.

(c) The bridge is rebalanced using C_a and C_b, and the C_b micrometer position, θ_b, is noted.

(d) C_{s10} is removed and the bridge rebalanced without altering C_b.

(e) Stages (b) to (d) are repeated to produce a set of contiguous points covering the whole operating range of C_b.

(f) The set of points obtained so far, which represent known changes of 1 bar capacitance against micrometer position, are then referred to an absolute value by setting C_b = 3.5 pF at θ_b = 0.825" (C_a = 3.0 pF at θ_a = 0.825" for the A arm). These values are based on Woods original estimates as derived in [A.I.D.] section 7.1 pages 17-20, the difference between the R.F. and A.F. capacitance values at $\theta_{(a \text{ or } b)}$ = 0.825" being significant.

(g) The calibration is completed by using cubic spline interpolation techniques to calculate the 1 bar capacitances required at intermediate micrometer positions.

Measurements of C_{s10} made over the 0.1" to 0.7" range of both C_a and C_b using the new calibration method gave maximum variations from the mean value of less than 0.1% of 100 MHz and 0.15% at 200 MHz which are adequately small for the accuracy requirements of the bridge. It should be noted in connection with section (f) above that absolute 1-bar capacitance values, in contrast to changes in them, are not required to any great precision since they only appear in residual bridge correction terms (ie. the term $+\omega^2 L_j(2\,\bar{C}_{b2}-\bar{C}_{a1}-\bar{C}_{a2}-C_5)$ in equation (15) of this report).

In order to assess the accuracy of the new calibration curves the standard capacitors C_{s11}, C_{s12} and C_{s13} (having nominal A.F. values of 5 pF, 10 pF and 20 pF respectively) were measured on the bridge at various initial positions on C_a and C_b and the results compared with the calculated values for the standards. Table 2 gives the assigned uncertainty figures resulting from this exercise.

TABLE 2

UNCERTAINTY OF MEASURING CAPACITORS C_a AND C_b

Frequency (MHz)	Uncertainty in C_a and C_b at 1 bar points (rectangular distribution semi-range)	Range of C_a and C_b over which uncertainty figure is valid
15	$\pm$ 0.10% $\pm$ 0.003 pf	0.1" to 0.7"
100	$\pm$ 0.15% $\pm$ 0.003 pF	0.1" to 0.7"
200	$\pm$ 0.3% $\pm$ 0.003 pF	0.1" to 0.7"

(ii) Inductance L_t and Capacitance C_t of the Bridge Terminals

These elements are measured using the technique described in [A.I.D.] section 18.4 pages 75-77 from which the values L_t = 2750 pH and C_t = 46 pF, both having an associated measurement uncertainty of ± 0.5%, are obtained.

(iii) Common Junction Equivalent Inductances L_j and L_k (both arms)

These residuals are measured using the methods described in [A.I.D.] sections 18.6 and 18.7 pages 77-83 from which the values L_j = 324 pH and L_k = 276 pH are obtained. The associated uncertainty limits have however been increased to ± 5% for both terms based on measurements made at RSRE by R.E. Spinney.

(iv) Shunt Conductances g_a and g_b

In the analysis of [A.I.D.] Appendix XVIII, the term $+2w^2L_jg_b\Delta\overline{C}_b$ (ie. the last term of the equation above equation (A5) is neglected as being insignificant although, as pointed out in a private communication from R.E. Spinney, this is not true for a g_b value in the order, as proves to be the case, of 1 mS or greater. This term, with appropriate sign, has therefore to be added to equation (15) of this report (and a similar term for the A arm in equation (17)). Also, none of the terms containing g_a and g_b in equations (15) to (18) have been neglected as suggested in the [A.I.D.] paragraph above equation (130).

The method developed by R.E. Spinney at RSRE to measure g_a and g_b is explained in Appendix 1, resulting in an associated uncertainty for both terms of ± 10%. Note that the value of g_a or g_b chosen is that when the bridge is initially balanced ie. without any device connected to the measurement terminal.

(v) Residuals R_{oa} and R_{ob} of the Precision Variable Capacitors C_a and C_b

In the method described in [A.I.D.] section 18.8 pages 83-84 the effect of the conductances g_a and g_b have been ignored. To allow for this, Appendix 2 describes a modification to this method developed by R.E. Spinney at RSRE which results in curves of equivalent conductance G_{ka} and G_{kb}, corresponding to R_{oa} and R_{ob} respectively, being derived as a function of the C_a and C_b related 1 bar capacitance values. This affects equations (15) to (18) by replacing all R_o terms with G_k terms based on the relationship

$$G_k = w^2R_o\overline{C}^2 \qquad (20)$$

The measurement uncertainty associated with both G_{ka} and G_{kb} is ± 10%.

(vi) Bridge Terminal Adaptors

Each bridge terminal is fitted with a brass adaptor, shown in cross section in fig. 9, to enable measurements to be made using the GR900 connector. Each device is characterised electrically by calculating the transmission line impedance of sections 1 and 2 as well as the fringing and step capacitances C_{fa}, C_{s1} and C_{s2} [4] based on mechanical measurements made in the RSRE Metrology Laboratory. An allowance is also made for skin

effect in the conductors by including a reciprocal velocity factor [3] calculated from theoretical conductivity values.

The procedure used to calculate the admittance of a DUT connected at the measurement plane allowing for the adaptor is given below.

(a) The susceptance of the adaptor fringe capacitance C_{fa}, which exists at initial bridge balance (ie the DUT not yet connected) is transformed through adaptor sections 1 and 2 and then the bridge terminals, each of the three stages represented using standard transmission line formulae and an allowance being made for the step capacitances C_{s1} and C_{s2}.

(b) The change in the 1 bar admittance value resulting from the connection of the DUT and calculated using the 1 bar balance difference equations, is then added to the admittance from stage (a) above.

(c) The admittance from stage (b) is transformed back through the bridge terminals and adaptor sections in a reverse process to stage (a), the resulting admittance being the actual value of the DUT itself.

The use of this procedure means that the term C_f in equations (16) and (18) of this report is no longer required.

8. CALIBRATION PROCEDURES FOR THE SERIES ELEMENTS

(a) Bridge Resistor R.F. Conductance Term, Zeta

This residual is measured using the technique of [A.I.D.] section 18.9 pages 84-85, and allows for the variation of the R.F. conductance G_s of the bridge resistor in terms of the relationship.

$$G_s = G_{ss}(1 + \text{Zeta})$$

where G_{ss} is the D.C. conductance of the resistor. The measurement method exploits the fact that for measurements made on the B arm the G_s term appears in the numerator of the balance difference equation unlike for the A arm where it appears in the denominator, (see equations (15) and (17)). If the same conductance is measured on both arms therefore, dividing one conductance result by the other will give the term $(1 + \text{Zeta})^2$ directly.

The uncertainty limits associated with Zeta are estimated to be $\pm$ 0.001 at 100 MHz and $\pm$ 0.0015 at 200 MHz.

(b) The Bridge Resistor Shunt Capacitance C_{sg}

This component is measured using the method described in [A.I.D.] section 18.5 pages 77-78 although it has been found simpler to find the term C_{sg}/G_s as a whole and not to separately isolate C_{sg}. The measurement procedure is similar to that used in section (a) above except that now the capacitance values obtained from each arm are subtracted from each other. This estimates the term $2.\overline{G}_x.\frac{C_{sg}}{G_s}$ from which, knowing an approximate value for $\overline{G}_x$, C_{sg}/G_s can be found.

The uncertainty limits associated with C_{sg}/G_s are estimated to be $\pm$ 0.0005 at 15 MHz, $\pm$ 0.001 at 100 MHz and $\pm$ 0.0015 at 200 MHz.

9. FINAL BALANCE DIFFERENCE EQUATIONS USED WITH THE RSRE TWIN T BRIDGE

The final balance difference equations at the 1 bar point, which differ slightly from those in equations (15) to (18) for reasons explained in section 7 of this report, are given below.

DUT connected to the B arm measurement terminals

$$\overline{G}_{xb} = \frac{G_s C_3}{C_1 C_2}\Delta\overline{C}_a \left\{ 1 + w^2 L_j(2\overline{C}_{b2}-\overline{C}_{a1}-\overline{C}_{a2}-C_5) - w^2 L_k(\Delta\overline{C}_a+C_5) \right.$$
$$\left. -2(L_j+L_k)\left(\frac{C_3 g_a G_s}{C_1 C_2} + \frac{w^2 C_1 C_2 g_b}{C_3 G_s}\right)\right\} + G_{kb1}-G_{kb2}-2w^2 L_j g_b \Delta\overline{C}_b \qquad (21)$$

$$\overline{C}_{xb} = \Delta\overline{C}_b + \overline{G}_{xb}\frac{C_{sg}}{G_s} + (L_j+L_k)\overline{G}_{xb}^{\,2} + 2(L_j+L_k)g_b\overline{G}_{xb} - 2L_k g_a \overline{G}_{xb}$$
$$- \frac{G_s C_3}{w^2 C_1 C_2}\left(1 + w^2\frac{C_{sg}^2}{G_s^2}\right)(G_{ka1}-G_{ka2}) \qquad (22)$$

DUT connected to the A arm measurement terminals

$$\overline{G}_{xa} = \frac{-w^2 C_1 C_2}{G_s C_3}\left(\frac{1}{1 + w^2\frac{C_{sg}^2}{G_s^2}}\right)\Delta\overline{C}_b \left\{ 1 + w^2 L_j(2\overline{C}_{a2}-\overline{C}_{b1}-\overline{C}_{b2}+C_5) + w^2 L_k(C_5-\Delta\overline{C}_b) \right.$$
$$\left. +2(L_j+L_k)\left(\frac{C_3 g_a G_s}{C_1 C_2} + \frac{w^2 C_1 C_2 g_b}{C_3 G_s}\right)\right\} + G_{ka1}-G_{ka2}-2w^2 L_j g_a \Delta\overline{C}_a \qquad (23)$$

$$\overline{C}_{xa} = \Delta\overline{C}_a - \overline{G}_{xa}\frac{C_{sg}}{G_s} + (L_j+L_k)\overline{G}_{xa}^{\,2} + 2(L_j+L_k)g_a\overline{G}_{xa} - 2L_k g_b \overline{G}_{xa}$$
$$- \frac{C_1 C_2}{G_s C_3}(G_{kb2}-G_{kb1}) \qquad (24)$$

When comparing equations (15) to (18) with equations (21) to (24) note that, in the latter, the following relationship has been used.

$$R_s = 1/G_s\left(1 + w^2 C_{sg}^{\,2}/G_s^{\,2}\right)$$

where $G_s = G_{ss}(1 + Zeta)$ and G_{ss} is the D.C. conductance of G_s.

10. ASSESSMENT OF BRIDGE MEASUREMENT UNCERTAINTY

In order to assess the overall bridge measurement uncertainty a computer program was written. This calculates the admittance of any measured D.U.T., ten times, each time increasing the value of one of the components of uncertainty, listed in Table 3, by its own associated uncertainty limit, and then returning its value to the nominal one, ready for the next calculation. The ten admittances obtained are then compared with their nominal value giving a set of percentage variations, each representing the effect of the rectangular distribution semi-range variation of the associated component. The 95% confidence limit of measurement uncertainty is then calculated [5] for both the conductive and suceptive components of the D.U.T. admittance.

TABLE 3

LIST OF COMPONENTS OF UNCERTAINTY CONTRIBUTING TOWARDS THE OVERALL BRIDGE MEASUREMENT UNCERTAINTY

Source of uncertainty	Associated limits (Semi-range of rectangular dist.)
Precision Variable Capacitors C_a and C_b	± 0.10% ± 0.003 pF at 15 MHz
	± 0.15% ± 0.003 pF at 100 MHz
	± 0.30% ± 0.003 pF at 200 MHz
Inductance of bridge terminals L_t	± 0.5%
Capacitance of bridge terminals C_t	± 0.5%
Common junction equivalent inductances L_j, L_k	± 5.0%
Shunt conductances g_a, g_b	± 10.0%
Conductances G_{ka}, G_{kb}	± 10.0%
Bridge r.f. conductance term, Zeta	Zero at 15 MHz
	± 0.001 at 100 MHz
	± 0.0015 at 200 MHz
C_{sg}/G_s	± 0.0005 at 15 MHz
	± 0.001 at 100 MHz
	± 0.0015 at 200 MHz

As mentioned in the introduction, the admittance of unknowns is measured in two parts; the conductance G_x, over a range from 0 to 50 mS, and capacitance C_x, over a range from 0 to 50 pF.

Standards measured on the bridge over the last eleven years fall into four categories as listed below.

(a) One-port capacitors. 1 to 20 pF

(b) One-port resistors. 33 ohms to 100 ohms

(c) Two-port resistors. 20 ohms to 1000 ohms
(One port terminated in a short circuit)

(d) Two-port resistors. 0.5 ohms to 10 ohms
(One port terminated in a 50 ohm load)

The random component of measurement uncertainty is negligible with GR900 connectors fitted to the bridge providing the connector contact faces are clean and great care is taken to avoid producing mechanical vibrations during the connect/disconnect cycle (including tightening the connector to the specified torque of 1.4 Nm using a torque spanner). The effect of mechanical vibrations on the bridge is to initiate mechanical relaxation on the shafts of the shunt capacitors C_{at} (60 pF), and C_{bt} (100 pF), which is sufficient to partially unbalance the bridge. A measurement procedure to eliminate this effect has been introduced.

The overall bridge uncertainty is a function of both frequency and the measured values of G_x and C_x. The uncertainty in capacity is further complicated by cross-terms involving G_x (as can be seen from equations (22) and (24)) so that a statement of bridge uncertainty in the form of a single equation, is necessarily only approximate. However, by using the measured values of the complete range of standards measured over the past eleven years a single equation of uncertainty has been produced for each frequency which is accurate to ± 0.15% in most cases. This is shown in table 4.

TABLE 4

SINGLE EQUATIONS OF TWIN T BRIDGE OVERALL MEASUREMENT UNCERTAINTY

Freq. MHz	Uncertainty in Conductance G_x mS. (95% CL)	Uncertainty in Capacitance C_x pF. (95% CL)
15	± 0.15% ± 0.005	± 0.01% ± 0.001.G_x(mS) ± 0.003
100	± 0.25% ± 0.005	± 0.17% ± 0.0013.G_x(mS) ± 0.003
200	± 0.5% ± 0.005	± 0.3% ± 0.0018 G_x(mS) ± 0.003

In practice when standards are calibrated the individual uncertainty in G_x and C_x is calculated by a computer program from the measured values for each standard, but the complex form of the bridge balance equations together with the minimum values of systematic uncertainty components, leads to overall bridge uncertainty figures which are not only dependent on the minimum values of G_x and C_x, but also on their ratio.

A better appreciation of the significance of this effect can be obtained from Tables 5 and 6, which list the range of uncertainties associated with standards having values of G_x and C_x within the ranges shown.

For example, from Table 6, a 1 pF capacitor having negligible G_x, has an uncertainty in C_x, in the range 0.49% to 0.7% at 200 MHz, but from Table 5 a standard having $G_x > 1$ mS and $C_x = 1$ pF can have an uncertainty in C_x of 4.5%.

TABLE 5

TRUE BRIDGE OVERALL UNCERTAINTY FIGURES FOR ALL STANDARDS HAVING A MINIMUM CONDUCTANCE AND CAPACITY OF 1 mS AND 0.15 pF RESPECTIVELY

CONDUCTANCE RANGE	UNCERTAINTY IN CONDUCTANCE % (95% CL)		
	15 MHz	100 MHz	200 MHz
1 - 2 mS	0.4 - 0.65	0.5 - 0.74	0.7 - 0.94
5 - 50 mS	0.17 - 0.25	0.28 - 0.35	0.5 - 0.64
CAPACITANCE RANGE	UNCERTAINTY IN CAPACITANCE % (95% CL)		
	15 MHz	100 MHz	200 MHz
0.15 - 1 pF	2 - 13	3 - 13	4.5 - 14
1 - 3 pF	0.3 - 2	0.4 - 3.1	0.6 - 4.5
> 3 pF	0.24 - 1	0.32 - 1.4	0.53 - 1.8

TABLE 6

TRUE BRIDGE OVERALL UNCERTAINTY FIGURES FOR STANDARD CAPACITORS

CAPACITANCE RANGE	UNCERTAINTY IN CAPACITY % (95% CL)		
	15 MHz	100 MHz	200 MHz
1 - 5 pF	0.21 - 0.45	0.28 - 0.51	0.49 - 0.71
> 5 pF	0.16 - 0.21	0.23 - 0.28	0.41 - 0.49

11. CONCLUSIONS

Since the XT-90 Twin T bridge was first built, some thirty years ago, a number of modifications have been made, the most recent being those made at RSRE to the measurement and calibration procedures. In particular the introduction of computer derived calibrations, using curve fitting techniques, has given greater calibration accuracy and extended the useful operating range of the measuring capacitors.

An assessment of the bridge systematic measurement uncertainty has been performed resulting in a definitive uncertainty figure calculated in terms of the 95% confidence probability limit.

12. REFERENCES

1. Woods, D. "A Precision V.H.F. Twin T Dual Admittance Bridge and Associated Standards", A.I.D. Report No. Rad.Elec./7, January 1950.

2. Clarke, R.N. "Notes on the Use and Theory of the XT-90 (Woods) Twin-T Dual Admittance Bridge", National Physical Laboratory Memorandum No. DES.24, December 1978.

3. Woods, D. "Immittance Transformation using Precision Air-Dielectric Coaxial Lines and Connectors", Proc. IEE, Vol. 118, No. 11, pp 1667-1674, November 1971.

4. Hodgetts, T.E. "The Calculation of the Equivalent Circuits of Coaxial-Line Step Discontinuities", RSRE Memorandum No. 3422, 1981.

5. Hinton, L.J.T. "Uncertainty and Confidence in Measurements", Lecture 19, IEE Fourth Vocation School on "RF Electrical Measurements", University of Lancaster, 8-14 July 1979.

APPENDIX 1 - METHOD FOR MEASURING THE SHUNT RESIDUALS g_a and g_b

The initial conductances g_a and g_b of the Twin T bridge result mainly from losses in the top block section, the settings of the latter being determined by the initial positions of C_a and C_b. The change of conductance with C_a or C_b can be measured on the bridge itself using the method described below (using the B arm as the example).

(a) Set C_b = 0.8", C_a = 0.4" and balance the bridge using the top block variable capacitances.

(b) Set C_b = 0.7" and balance the bridge using C_a and the B arm top block variable capacitances, taking care not to disturb the A arm top block controls. The change in g_b is calculated from the change in C_a position using the 1 bar balance difference equations.

(c) Reset C_a = 0.4" and repeat stages (a) and (b) above but with the C_b values reduced by 0.1". This process is continued over the whole C_b operating range producing a set of points representing changes in g_b with C_b position. Cubic spline techniques are then used to calculate intermediate g_b values.

The total conductance associated with each arm is then measured using the resonance method described below, the B arm again being used as the example.

(a) The bridge is balanced in order to obtain the correct relationship between the top block setting and C_b.

(b) The input and output leads are unplugged and shorting plugs are inserted into the input and output sockets in order to electrically isolate the A and B arms from each other.

(c) If the B arm conductance is being measured, the bridge resistor is removed.

(d) The circuit of fig. 10 is set up where C_1 and C_2 are provided by specially adapted GR874 type connectors, one of which couples to the B arm bridge terminal, the other to the B arm junction block through the upper hole in the bridge front face.

(e) The attenuator is set to 13 dB and C_b adjusted to give maximum response on the receiver.

(f) The attenuator setting is reduced to 10 dB and C_b adjusted each side of the maximum to give the same receiver output as in stage (e).

(g) The required conductance is equal to 0.5 x the total susceptance change in stage (f).

Now that g_b is known for a particular setting of C_b, the curve of changes in g_b, obtained from the first experiment can be expressed in absolute terms.

THEORY OF RESONANCE METHOD

The circuit of fig. 10 is set up with $C_1 = C_2 = C$ where $C < 0.1$ pF in order to prevent significant loss being coupled in from either the source or the load. Also, for convenience, we define

$$X = \frac{-1}{WC}$$

and $Z = R + R + jX$

where $R = 50\ \Omega$ is the impedance of both the source and load (attenuator).

B is equal to the sum of the precision variable capacitor susceptance and the top block susceptance. From the transfer impedance of a T network.

$$V = R.e/[2(R+jX) + (R+jX)^2(G+jB)] \qquad A1(1)$$

Defining $D = 2(R+jX) + (R+jX)^2(G+jB)$ ie the denominator of equation A1(1)

then $D = 2R+j2X + (R^2-X^2)G-2RXB+j(R^2-X^2)B + j2RXG$

$$= 2R + (R^2-X^2)G-2RXB +j[B(R^2-X^2)+2RXG+2X]$$

$$\therefore |D'|^2 = [2R+(R^2-X^2)G-2RXB]^2 + [2X+B(R^2-X^2)+2RXG]^2$$

$$= 4R^2+(R^2-X^2)^2G^2+4R^2X^2B^2+4R(R^2-X^2)G-8R^2XB-4RXB(R^2-X^2)G$$

$$+ 4X^2+(R^2-X^2)^2B^2+4R^2X^2G^2+4X(R^2-X^2)B+8RX^2G+4RXB(R^2-X^2)G$$

$$= 4(R^2+X^2)+(R^2+X^2)G^2+(R^2+X^2)^2B^2+2G(2R^3-2RX^2+4RX^2)+2B(-2X^3+2R^2X-4R^2X)$$

$$\therefore |D|^2 = (R^2+X^2)^2B^2-4BX(R^2+X^2)+(R^2+X^2)^2G^2+4GR(R^2+X^2)+4(R^2+X^2)$$

$$= |Z|^4B^2-4BX|Z|^2+|Z|^4G^2+4GR|Z|^2+4|Z|^2$$

$|D|^2$ will be a minimum when $\frac{d|D|^2}{dB} = 0$ (ie a <u>minimum</u> because $|D|^2 \to \infty$ when $|B| \to \infty$)

Now $\frac{d|D|^2}{dB} = 2|Z|^4B - 4X|Z|^2$

$\therefore \quad 2|Z|^4B = 4X|Z|^2$ for $\frac{d|D|^2}{dB} = 0$

ie when $B = \frac{2X}{|Z|^2}$

$\therefore$ Minimum value of $|D|^2 = 4X^2-8X^2+|Z|^4G^2+4GR|Z|^2+4|Z|^2$

$$= |Z|^4G^2+4GR|Z|^2+4|Z|^2-4X^2$$

Now $wC < 0.1$ mS ie $|X| > 10$ KΩ and R = 0.05 KΩ

$\therefore$ $|Z|^2 = X^2$ with an error of less than 0.0025%

$\therefore$ Minimum value of $|D|^2 = |Z|^4G^2+4GR|Z|^2$

Now $|D|^2$ will be equal to twice its minimum value (ie $V = Vmax/\sqrt{2}$) when

$$|Z|^4B^2-4BX|Z|^2+|Z|^4G^2+4GR|Z|^2+4|Z|^2 = 2|Z|^4G^2+8GR|Z|^2$$

ie when $|Z|^4B^2-4BX|Z|^2-|Z|^4G^2-4GR|Z|^2+4|Z|^2 = 0$

ie $$B^2 - \frac{4BX}{|Z|^2} - G^2 - \frac{4GR}{|Z|^2} + \frac{4}{|Z|^2} = 0$$

$$B = \frac{2X}{|Z|^2} \pm \sqrt{\frac{4X^2}{|Z|^2} + G^2 + \frac{4GR}{|Z|^2} - \frac{4}{|Z|^2}}$$

$$B = \frac{2X}{|Z|^2} \pm G\sqrt{1 + \frac{4R}{|Z|^2G}} \quad \text{since} \quad \frac{X^2}{|Z|^4} \approx \frac{1}{|Z|^2}$$

$$= \frac{2X}{|Z|^2} \pm G(1 + \alpha) \text{ where } \alpha < \frac{0.001}{G}$$

For G of the order of 1 mS, which proves to be the case, α can be neglected.

$\therefore$ $$\underline{B = \frac{2X}{|Z|^2} \pm G}$$

APPENDIX 2 - MODIFIED METHOD FOR MEASURING RESIDUALS R_{oa} and R_{ob}

When the conductances g_a and g_b are included in the method described in [A.I.D.] section 18.8 pages 83-84, equation (176) becomes (using the B arm as an example)

$$\overline{G}_x = \frac{w^2 R_t C_x (C_x + C_t)}{(1 - w^2 L_t C_x)} - w^2 R_{ob} (\overline{C}_{b1}^2 - \overline{C}_{b2}^2) + 2w^2 L_j g_b (\overline{C}_{b1} - \overline{C}_{b2})$$

and the curve to be plotted is

$$\Delta G' = \Delta \overline{G} - 2w^2 L_j g_b (\overline{C}_{b1} - \overline{C}_{b2}) \text{ against } (\overline{C}_{b1}^2 - \overline{C}_{b2}^2) \qquad \text{A2(1)}$$

The results of this experiment showed that a constant R_{ob} value exists for lower values of $\overline{C}_b$ but that at the top end the losses increase more rapidly. Because [A.I.D.] equation (117) is no longer strictly valid for a variable R_{ob}, it was decided to derive a graph of equivalent conductance G_{kb} against C_b by using the relationship

$$\overline{C}_{b1}^2 - \overline{C}_{b2}^2 = \overline{C}_x (2\overline{C}_{b2} + \overline{C}_x) \text{ where } \overline{C}_x = \overline{C}_{b1} - \overline{C}_{b2} \qquad \text{A2(2)}$$

where $\overline{C}_x$ is known from the bridge measurements. Then over the range where R_{ob} is constant, $G_{kb} = w^2 R_{ob} \overline{C}_b^2$ from [A.I.D.] equation (117) and since R_{ob} is now known, a parabola of G_{kb} against $\overline{C}_b$ can be drawn. To extend this curve, a point $(\overline{C}_{b2}, G_{kb2})$ is taken at its top end, $(\overline{C}_{b1}^2 - \overline{C}_{b2}^2)$ is calculated from equation A2(2) and the conductance change between points $\overline{C}_{b2}$ and $\overline{C}_{b1}$ found using the original graph obtained from equation A2(1). This process is continued until the whole operating range of the capacitor C_b has been covered.

The measurement is made at a frequency of 200 MHz and the value of G_k at any other frequency calculated using the relationship derived below.

Assuming that R_o varies with the square root of frequency then

$$R_{of} = R_{200} \sqrt{\frac{f}{200}} \qquad \text{A2(3)}$$

where R_{of} is the value of R_o at frequency f (MHz)

R_{200} is the value of R_o at frequency 200 MHz

Also $G_{kf} = (2\pi)^2 f^2 R_{of} \overline{C}^2$ from equation (20) .... A2(4)

where G_{kf} is the value of G_k at frequency f (MHz).

Therefore from A2(3) and A2(4)

$$G_{kf} = (2\pi)^2 f^2 R_{200} \sqrt{\frac{f}{200}}\ \overline{C}^2 \qquad \text{A2(5)}$$

But $G_{k200} = (2\pi)^2 200^2 R_{200} \overline{C}^2$ from A2(5) A2(6)

where G_{k200} is the value of G_k at frequency 200 MHz.

Therefore from A2(5) and A2(6)

$$G_{kf} = (2\pi)^2 f^2 \sqrt{\frac{f}{200}} \cdot \frac{G_{k200}}{(2\pi)^2 200^2}$$

$$= \underline{G_{k200} \left(\frac{f}{200}\right)^{\frac{5}{2}}} \quad \text{A2(7)}$$

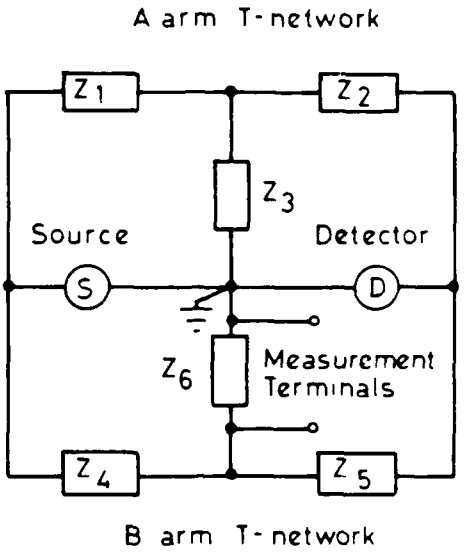

FIG 1 BASIC BRIDGE CIRCUIT CONFIGURATION

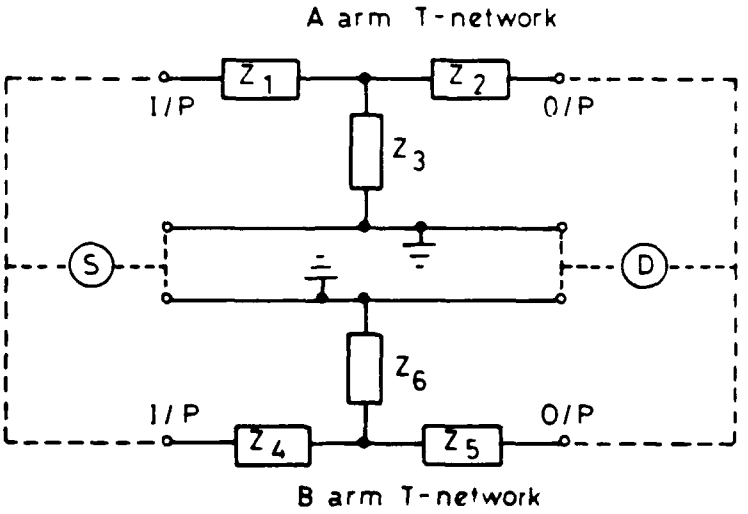

– – – – indicates connections creating the Twin T Bridge circuit from two separate T-networks

FIG 2 BASIC CIRCUIT AS CONNECTION OF TWO T – NETWORKS

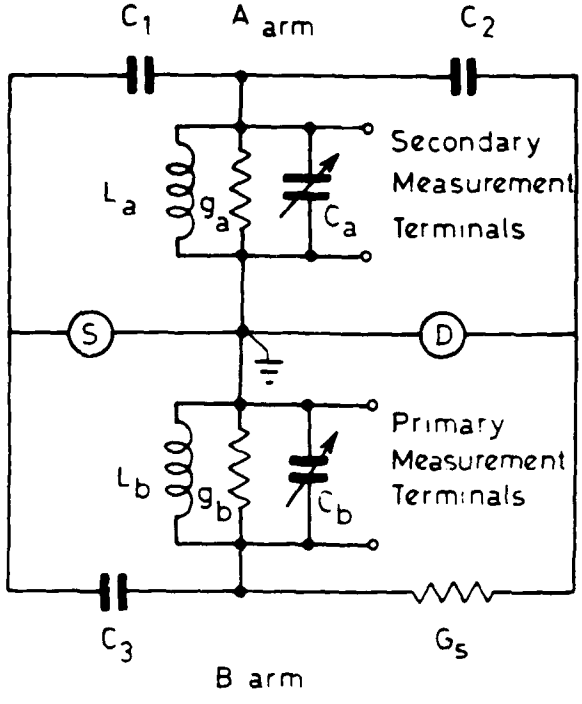

C_1 = 5pF G_s = 5mS (200Ω)

C_2 = 5pF Range of C_a = 25pF

C_3 = 10pF Range of C_b = 50pF

FIG 3 BASIC CIRCUIT COMPONENTS

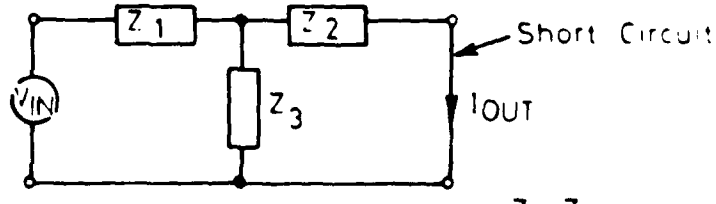

$$Z_{ta} = \frac{V_{IN}}{I_{OUT(S/C)}} = Z_1 \cdot Z_2 \cdot \frac{Z_1 Z_2}{Z_3}$$

FIG 4 TRANSFER IMPEDANCE OF "A" ARM

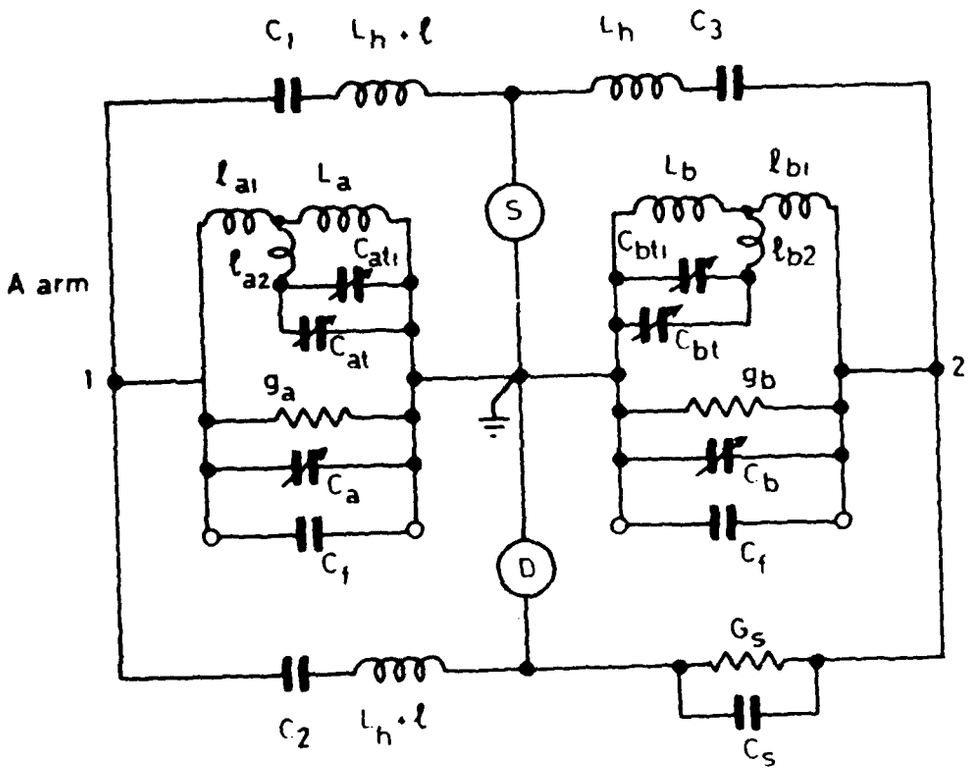

C_{at} = 60 pF

C_{bt} = 100pF

C_{at1} = 0.7pF trimmer

C_{at1} = 0.7pF trimmer

FIG 5 FIRST STAGE TOWARDS PRACTICAL CIRCUIT

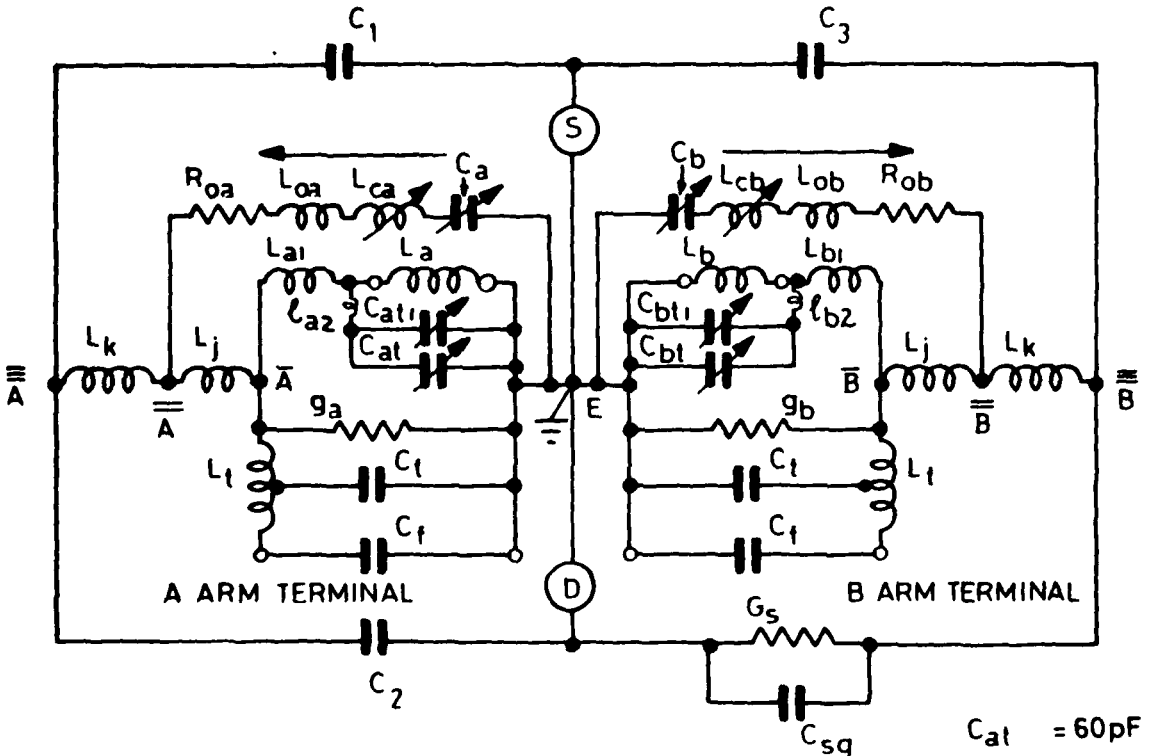

C_1 5pF
C_2 5pF
C_3 10pF
C_a 25pF variable
C_b 50pF variable

C_{at} = 60pF variable
C_{ati} = 0.7pF trimmer
C_{bt} = 100pF variable
C_{bti} = 0.7pF trimmer
G_s = 5mS (200Ω)

FIG 6 COMPLETE WOODS EQUIVALENT CIRCUIT

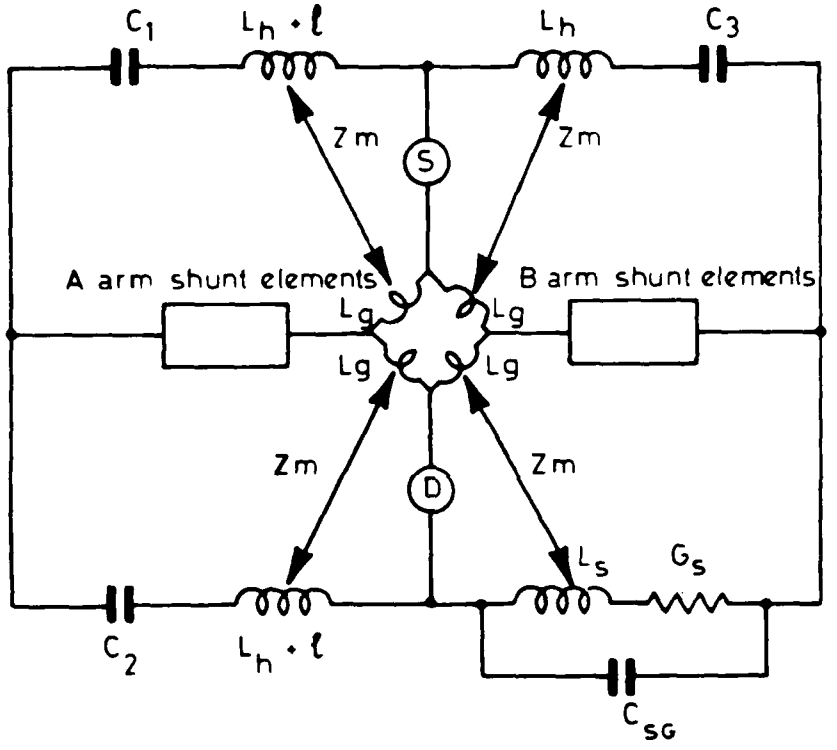

FIG 7 EFFECT OF COMMON AND MUTUAL EARTH IMPEDANCES

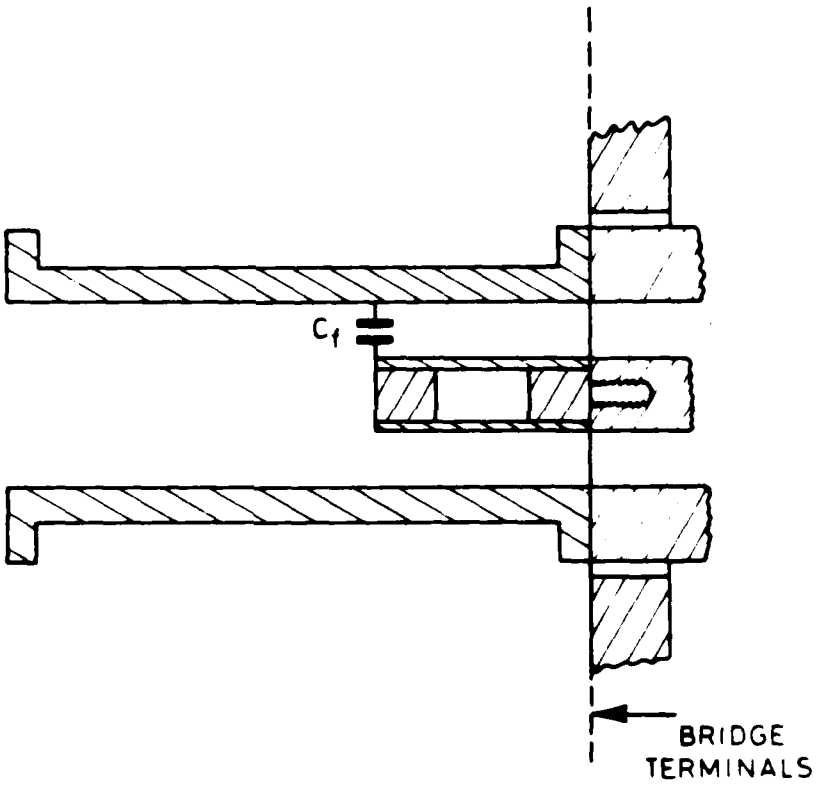

FIG 8 REVISED CONFIGURATION OF STANDARD CAPACITORS

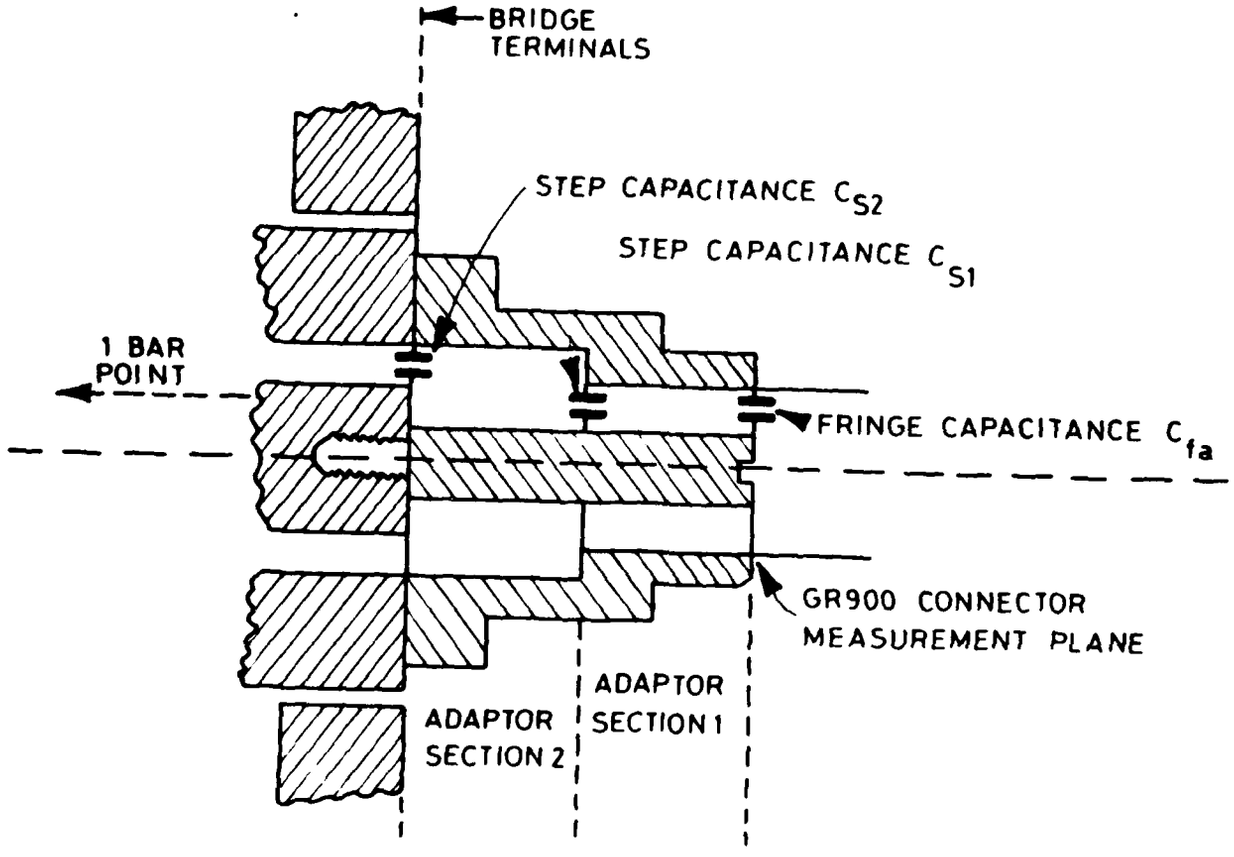

FIG 9 BRIDGE ADAPTOR TO GR900 CONNECTOR

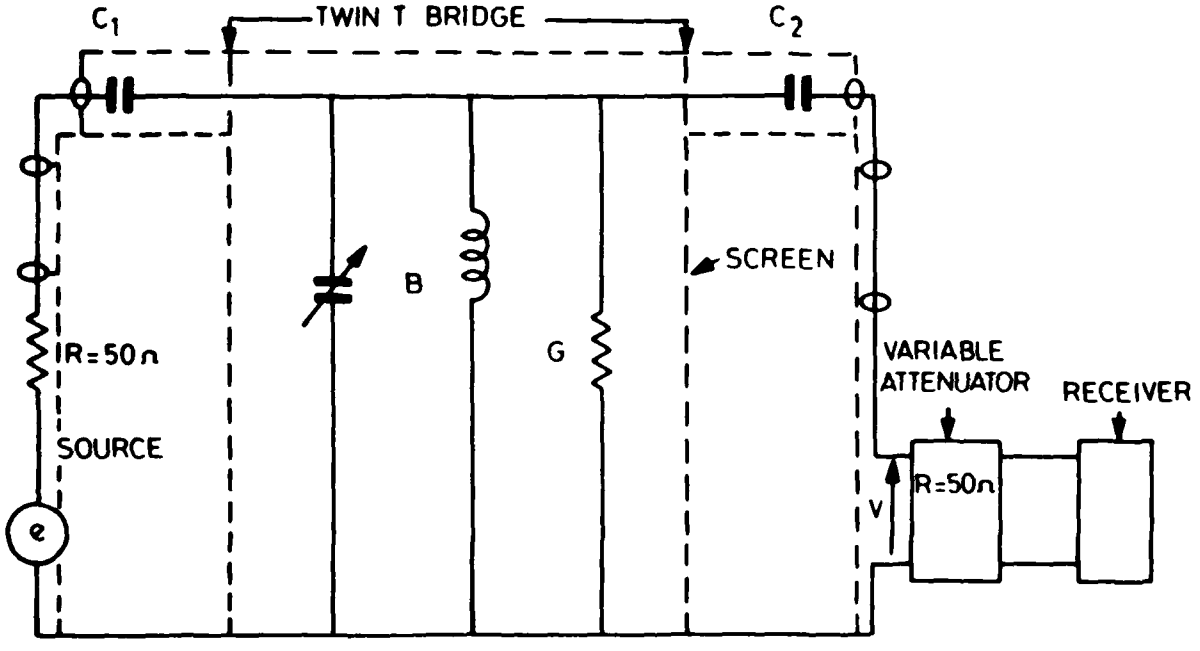

FIG.10. CIRCUIT ARRANGEMENT FOR MEASURING SHUNT RESIDUALS g_a AND g_b

DOCUMENT CONTROL SHEET

Overall security classification of sheet ..... Unclassified .....

(As far as possible this sheet should contain only unclassified information. If it is necessary to enter classified information, the box concerned must be marked to indicate the classification eg (R) (C) or (S))

1. DRIC Reference (if known)	2. Originator's Reference	3. Agency Reference	4. Report Security Classification
	Memo 3632		u/c

5. Originator's Code (if known)	6. Originator (Corporate Author) Name and Location
	ROYAL SIGNALS AND RADAR ESTABLISHMENT

5a. Sponsoring Agency's Code (if known)	6a. Sponsoring Agency (Contract Authority) Name and Location
	N/A

7. Title A REASSESSMENT OF THE MEASUREMENT UNCERTAINTY OF THE XT-90 TWIN T DUAL ADMITTANCE BRIDGE

7a. Title in Foreign Language (in the case of translations)

7b. Presented at (for conference papers) Title, place and date of conference

N/A

8. Author 1 Surname, initials	9(a) Author 2	9(b) Authors 3,4...	10. Date	pp. ref.
SLACK G J	GRAHAM T N W			

11. Contract Number	12. Period	13. Project	14. Other Reference

15. Distribution statement

UNLIMITED

Descriptors (or keywords)

continue on separate piece of paper

Abstract AS SUMMARY

END

DATE
FILMED

4-84

DTIC